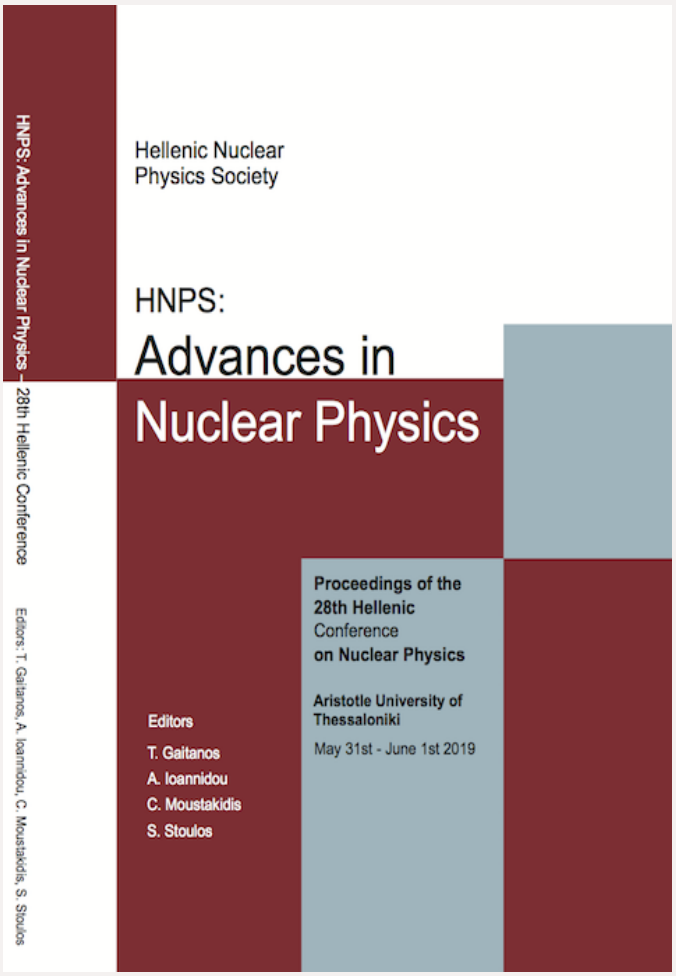
ePublishing

ΕΘΝΙΚΟ ΚΕΝΤΡΟ ΤΕΚΜΗΡΙΩΣΗΣ
EKT NATIONAL DOCUMENTATION CENTRE

HNPS Advances in Nuclear Physics

Vol. 27, 2019



Investigation of Photon Attenuation Properties of CR-39 Lens

Eke Canel — Akdeniz University, Faculty of Education, Department of Mathematics and Science Education, Division of Physics Education, 07058, Antalya, Turkey

Yildirim A. — Akdeniz University, Faculty of Science, Department of Physics, 07058, Antalya, Turkey

http://dx.doi.org/10.12681/hnps.2475

Copyright © 2019 Canel EKE, A. Yildirim

CC BY NC SA

To cite this article:

Eke, & Yildirim (2019). Investigation of Photon Attenuation Properties of CR-39 Lens. HNPS Advances in Nuclear Physics, 27, 60-67.

http://epublishing.ekt.gr | e-Publisher: EKT | Downloaded at 20/09/2021 19:03:40 |

HNPS Advances in Nuclear Physics vol. 27, pp. 60–67 (2020)
HNPS2019
doi:10.12681/hnps.2475

Investigation of Photon Attenuation Properties of CR-39 Lens

C. Eke[1] , A. Yildirim[2]

[1] *Akdeniz University, Faculty of Education, Department of Mathematics and Science Education, Division of Physics Education, 07058, Antalya, Turkey*
[2] *Akdeniz University, Faculty of Science, Department of Physics, 07058, Antalya, Turkey*

Abstract *The purpose of this study is to investigate photon attenuation parameters of Colombia Resin-39 (CR-39) lens, which are linear attenuation coefficient (LAC), mass attenuation coefficient (MAC), half value layer (HVL), tenth value layer (TVL), mean free path (MFP), effective atomic number (Z_{eff}) and effective electron density (N_{eff}). MACs were determined theoretically and with simulation in the energy range from 0.01 to 10^5 MeV. Also, obtained MACs of CR-39 lens were compared with MACs of pure aluminum and lead. Theoretically obtained Z_{eff} values were compared with Z_{eff} results obtained by the computer software.*

The results of this study are; a) the theoretically obtained MACs values are in agreement with MACs obtained results from simulation software, b) the theoretically obtained Z_{eff} values are in agreement with Z_{eff} obtained by the computer software c) the MACs of CR-39 lens are much lower than MACs of pure lead whereas there is not too much differences between MACs of CR-39 and pure aluminium d) the HVLs, TVLs and MFPs rise with increasing photon energy while the LACs and MACs reduce with increasing photon energy.

Keywords *mass attenuation coefficient, gamma–ray spectrometry, CR-39 lens*

Corresponding author: C. Eke (ceke@akdeniz.edu.tr) | *Published online:* May 1st, 2020

INTRODUCTION

Exploring the gamma–ray properties of the different materials and compounds are significant because gamma–rays are used in various objectives such as nuclear power plants, radiation dosimetry, medicine, industry, shielding, *etc.* [1-4]. Protection from the ionizing radiation effect is necassary for the humans because it causes distortion on the biological, atomic, molecular structure of the materials [5].

Gamma-rays interact with matter as photoelectric effect, Compton scattering and pair production and it depends on incident photon energy and structure of the absorber material. Photoelectric effect is dominant at low gamma-ray energies whereas pair production is dominant at high gamma-ray energies especially greater than 1022 keV. Compton scattering is prominent in the mid-photon energy range [6].

The gamma–ray attenuation parameters which are linear attenuation coefficient (LAC), mass attenuation coefficient (MAC), total atomic cross section (σ_a), total electron cross section (σ_e), effective atomic number (Z_{eff}) and effective electron density (N_{eff}), half value layer (HVL), tenth value layer (TVL), mean free path (MFP) are significant to decide the effects of the gamma-rays in matter [7]. These parameters can be determined by experimentally, theoretically and computer simulation [8,9].

The attenuation parameters of many different materials such as soil, oil-soil samples [10], raw wood and binderless particleboards of Rhizophora spp. [11], carbohydrates, (Esculine, Sucrose, Sorbitol, D–Galactose, Inositol, D–Xylose) [12], some vitamins (retinol, beta–carotene, thiamine, riboflavin, niacinamide, pantothenic acid, pyridoxine, biotin, folic acid, cyanocobalamin, ascorbic acid, cholecalciferol, alpha–tocopherol, ketamine, hesperidin) [13], some building materials [14], different

Licensed under a Creative Commons Attribution-NonCommercial-NoDerivatives 4.0 International License.

http://epublishing.ekt.gr | e-Publisher: EKT | Downloaded at 20/09/2021 19:03:40 |

types of glasses [15-17], some polymers (polyoxymethylene, poly acrylonitrile, natural rubber, polyethyl acrylate, polyphenyl methacrylate, and polyethylene tetraphthalate) [18-20], plastic [20-21] have been investigated in the scientific literature by the researchers.

In this study, Columbia Resin 39 (CR-39) plastic polymer having chemical composition $C_{12}H_{18}O_7$ which is called allyl diglycol carbonate [22-24] was investigated. CR–39 is generally used for nuclear reaction physics, radon dosimetry, radiobiological measurements as nuclear track dedectors and production of the eyeglass lenses [24,25].

The aim of this study is to investigate attenuation parameters of gamma radiation which are MACs, LACs, HVLs, TVLs, MFPs, atomic cross section, electron cross section Z_{eff} and N_{eff} of the CR-39 lens. The theoretically obtained MACs of CR–39 lens have been compared with the MACs obtained by the simulation code. Also theoretically obtained MACs of CR–39 lens have been compared with MACs of the Aluminium and lead. Theoretically obtained Z_{eff} values have been compared Z_{eff} values obtained by the computer software.

THEORETICAL CALCULATIONS

The linear attenuation coefficient (LAC) and mass attenuation coefficient (MAC) of CR–39 lens were calculated using the Beer Lambert law as following equations [6]:

$$I = I_0 e^{-\mu x} \tag{1}$$

$$\mu_m = \frac{\mu}{\rho} \tag{2}$$

where μ and μ_m are LAC and MAC of the absorber, respectively, x is the thickness of the sample, ρ is the density of the absorber, I is counts of per seconds of point sources with absorber and I_0 is counts of per seconds of point sources without absorber.

The MACs are calculated for mixtures and components considering basic ingredients of the absorber by using following equation [26]:

$$\mu_m = \frac{\mu}{\rho} = \sum_i w_i \left(\frac{\mu}{\rho}\right)_i \tag{3}$$

where w_i is the weight fraction of the atomic components and $\left(\mu/\rho\right)_i$ is the MAC of the i^{th} element. $\left(\mu/\rho\right)_i$ at all the absorption edges of all the components of the elements are calculated using interpolation for the atomic photoeffect cross section, coherent (Rayleigh) and the incoherent (Compton) scattering cross sections, cross sections for electron-positron production in the fields of the nucleus and of the atomic electrons also including the photoeffect cross sections for the individual atomic subshells [26].

In this study MACs of the CR-39 lens were calculated theoretically using WinXCom software [27]. WinXCom is Windows version of XCOM which was developed by the Berger and Hubbell [28] for computing MACs or photon interaction cross-sections for any element, compound or mixture at energies from 1 keV to 100 GeV [27].

In following equation 4 and 5 represent total atomic cross section per atom σ_a $(\mathrm{cm}^2/\mathrm{atom})$ and total electronic cross section per electron $\sigma_e(\mathrm{cm}^2/\mathrm{electron})$;

Licensed under a Creative Commons Attribution-NonCommercial-NoDerivatives 4.0 International License.

http://epublishing.ekt.gr | e-Publisher: EKT | Downloaded at 20/09/2021 19:03:40 |

$$\sigma_a = \frac{1}{N}\frac{\left(\mu/\rho\right)_{material}}{\sum_i \frac{w_i}{A_i}} \tag{4}$$

$$\sigma_e = \frac{1}{N}\sum_i \frac{f_i A_i}{Z_i}\left(\frac{\mu}{\rho}\right)_i \tag{5}$$

where N is the Avogadro's number, A_i is the atomic weight of the i^{th} element, w_i is fractional weight, f_i is the molar fraction of the i^{th} element and Z_i is the atomic number of the i^{th} element [3,11].

Effective atomic number Z_{eff} is calculated using following equation [3,11]:

$$Z_{eff} = \frac{\sigma_a}{\sigma_e} \tag{6}$$

Effective electron density N_{eff} $(\mathrm{electron/g})$ is related with (Z_{eff}) and it is calculated using following equation [3,11]:

$$N_{eff} = \frac{\left(\mu/\rho\right)_{material}}{\sigma_e} \tag{7}$$

The HVL, TVL and MFP are calculated as follows [29,30]:

$$HVL = \frac{ln2}{\mu} \tag{8}$$

$$TVL = \frac{ln10}{\mu} \tag{9}$$

$$MFP = \frac{1}{\mu} \tag{10}$$

SIMULATION PROCEDURE

Geant4 simulation toolkit is used for the simulation of mass attenuation coefficients [31-33]. Geant4 is a very powerful simulation software and currently used by many researchers around the world. It is one of the best simulation programs to investigate the particles passing through matter. It is used in the areas of nuclear physics, high energy physics, accelerator physics, medical physics and space sciences. There are many collaborators still developing the software. Research groups also create libraries for their own works which are contribute the developing of the toolkit. For this study Livermore library (Low Energy Electromagnetic Physics), which is an official Geant4 library, was used to determine the mass attenuation coefficients.

Using Geant4, one can calculate the attenuation coefficients by either directly from desired material or simply creating the experiment conditions and counting photons that reached the detector via code blocks. For both cases the results are almost the same. In this study we used the latter one. The lens and the detector are shown in Fig. 1.

In Fig. 1, the green cylinder is the lens sample and the blue cylinder is the HPGe detector. The axes are shown with arrows. Like a real experiment, simulations were done with and without the sample to calculate the attenuation coefficients. In Fig. 2, it is shown the gamma-ray interactions with the sample and the detector. Gamma–rays are propagating along all space from a point source. The source is placed just in front of the sample. The simulation was taken place in air. There is nothing else in the simulation setup for the gamma rays to interact and change the results.

Obtained results were discussed in the next section along with the theoretical ones.

Licensed under a Creative Commons Attribution-NonCommercial-NoDerivatives 4.0 International License.

http://epublishing.ekt.gr | e-Publisher: EKT | Downloaded at 20/09/2021 19:03:40 |

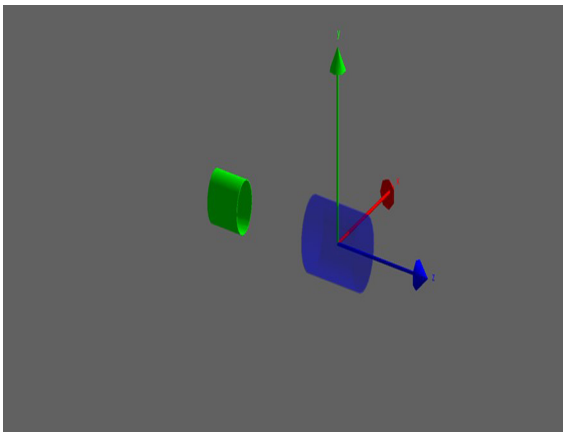


Figure 1. *Graphical demonstration of experiment setup*

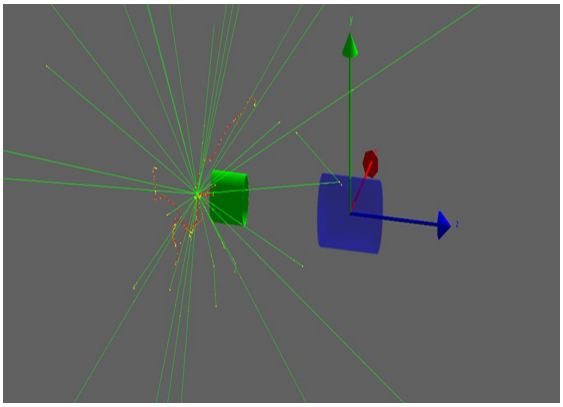


Figure 2. *The point source and the interactions of gamma rays with sample and detector*

RESULTS AND DISCUSSION

The variation of LACs and comparison MACs between WinXCom [27] and Geant4 [31-33] of CR-39 lens are shown in Fig. 3 and Fig. 4, respectively. Also, obtained MACs of CR-39 were compared the MACs of pure aluminum (*Al*) and lead (*Pb*) which are commonly used as shielding materials (see Fig. 5).

The MAC gives information about evaluating of the mean number of the interactions between incident photons and material which take place in a dedicated mass-per-unit field thickness of the investigated matter. The MAC is free of the density and physical situation of the absorber therefore it is more significant than the LAC [20]. As shown in Fig. 3, 4 and 5, the LACs and MACs decrease with increasing photon energy and it tends to be stable at higher photon energies because photoelectric effect is dominant at low photon energies, Compton scattering takes place at intermediate photon energies whereas pair production replaces at higher photon energies [7]. The theoretically obtained MACs by using WinXCom are agreement with obtained MACs by the Geant4 simulation software (see Fig. 2). The MACs of CR-39 are agreement with *Al* whereas the MACs of CR-39 are lower than *Pb* especially at low and high photon energies as shown in Fig. 5.

Licensed under a Creative Commons Attribution-NonCommercial-NoDerivatives 4.0 International License.

http://epublishing.ekt.gr | e-Publisher: EKT | Downloaded at 20/09/2021 19:03:40 |

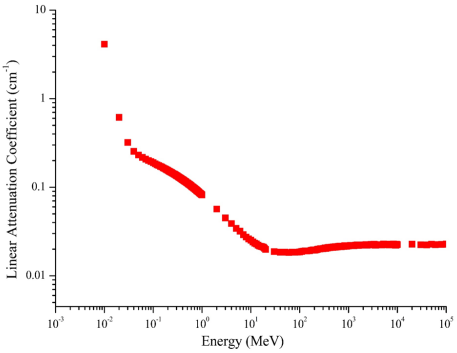


Figure 3. *Variation of LACs versus photon energies*

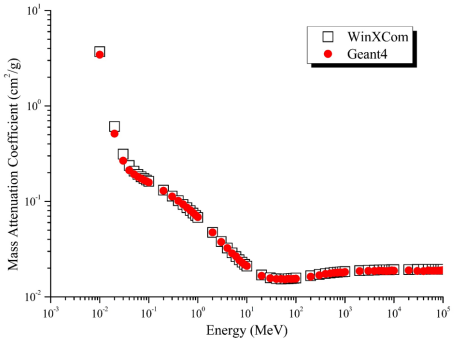


Figure 4. *Variation of MACs versus photon energies*

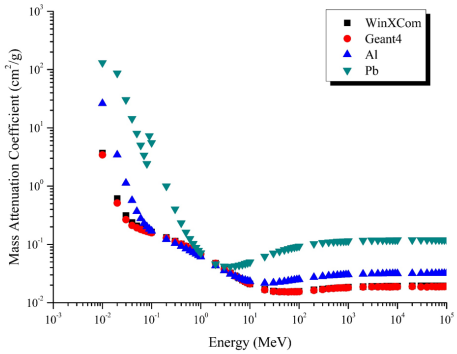


Figure 5. *Comparison of MACs of CR-39, Al and Pb versus photon energies*

Variations of HVLs, TVLs and MFPs versus photon energies as shown in Fig. 6. The HVL, TVL anf MFP of CR–39 increase with increasing photon energies. The HVL and TVL are described as the thickness of the absorber which decreases the intensity by a foctor of two and ten, respectively which are required for the radiation dosimetry evaluations. The MFP is average distance of a two successive

Licensed under a Creative Commons Attribution-NonCommercial-NoDerivatives 4.0 International License.

http://epublishing.ekt.gr | e-Publisher: EKT | Downloaded at 20/09/2021 19:03:40 |

photons where reduces 63% of the total intensity will interact [30]. The HVL and TVL of the absorber should be small for the strong radiation shielding [29].

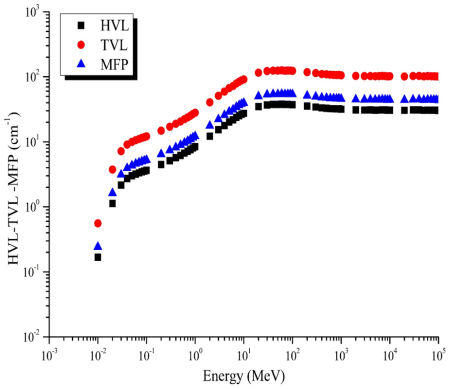


Figure 6. *Variation of HVLs, TVLs and MFPs versus photon energies*

Z_{eff} and N_{eff} are used to define for the compounds and mixtures because the atomic number of compounds and mixtures can not decribes with single atomic number against to incident photon energy. N_{eff} anf Z_{eff} (see Fig. 7 and Fig. 9) depend on the incident photon energy also Z_{eff} is ratio of the total electron cross section to total electronic cross section and N_{eff} is the number electrons per unit mass [5-34].

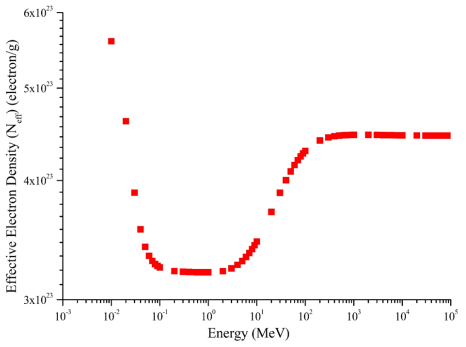


Figure 7. *Variation of effective electron densities versus photon energies*

Variation of effective electron density, total atomic cross section, total electronic cross section and effective atomic number versus photon energies are presented in Fig. 7, 8 and 9, respectively. The Z_{eff} values obtained using MACs values from WinXCom are agreement with obtained Z_{eff} values from AutoZeff software [35]. The N_{eff} and Z_{eff} sharply decreases at low photon energies, it tends to be stable at intermediate energies then these parameters increase again and tends to be constant at higher photon energies. The reason of this process is interaction of photons with matter as photelectric effect, Compton scattering and pair production. Especially, intermediate photon energies Compton scattering is effective and cross section of the Compton scattering varies linearly with atomic number [5].

Licensed under a Creative Commons Attribution-NonCommercial-NoDerivatives 4.0 International License.

http://epublishing.ekt.gr | e-Publisher: EKT | Downloaded at 20/09/2021 19:03:40 |

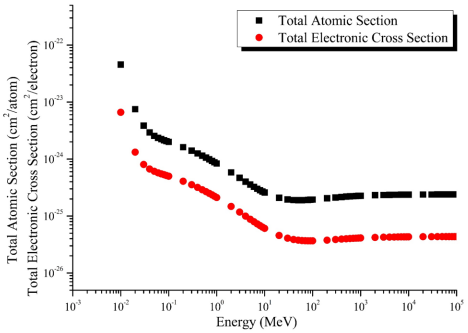


Figure 8. *Variation of total atomic cross section and total electron cross section versus photon energies*

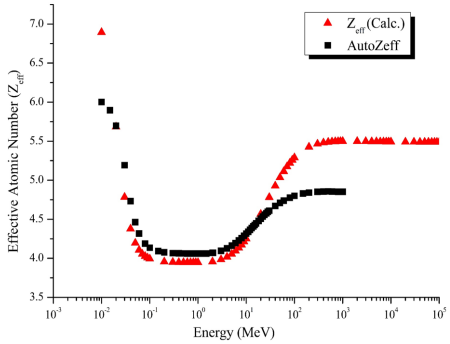


Figure 9. *Variation of effective atomic numbers versus photon energies*

CONCLUSIONS

In this study, radiation shielding parameters which are LACs, MACs, HVL, TVL, MFP, Z_{eff} and N_{eff} were calculated. The MACs were determined theoretically and with simulation in the energy range from 0.01 to 10^5 MeV. It was concluded that theoretically obtained MACs values of CR–39 lens were agreement with values obtained from Geant4 simulation software. The MACs of CR–39 lens were nearly equal to MACs of aliminum. The MACs of CR-39 lens were nearly equal to MACs of Aluminum though these values were lower than MACs of lead. The LACs, MACs, total atomic cross section and total electronic cross section decrease with increasing photon energies whereas HVLs, TVLs and MFPs rise with increasing photon energies. Theoretically obtained Z_{eff} values were compared with Z_{eff} values obtained from AutoZeff software. It was deduced that theoretically calculated Zeff values are close to obtained Z_{eff} values from AutoZeff software especially low and medium photon energies but there was significant differences at higher than 100 MeV.

In the future, the LACs and MACs can be calculated as experimentally and obtained results can be compared with theoretical and simulation results of CR–39 lens.

Licensed under a Creative Commons Attribution-NonCommercial-NoDerivatives 4.0 International License.

http://epublishing.ekt.gr | e-Publisher: EKT | Downloaded at 20/09/2021 19:03:40 |

HNPS Advances in Nuclear Physics vol. 27, pp. 60–67 (2020)

References

[1] A.Y. Abdel-Haseib et al., Journal of Nuclear Radiation and Physics, 13, 81 (2018).
[2] S. Gowda et al., Pramana-J. Phys. 63, 529 (2004), doi: 10.1007/BF02704481
[3] S.R. Manohara et al., Nucl. Instr. Meth. Phys. Res. B. 264, 9 (2007), doi:10.1016/j.nimb.2007.08.018
[4] R. Biswas et al., J. Radiat. Res. Appl. Sc. 9, 26 (2016), doi: 10.1016/j.jrras.2015.08.005
[5] N. Abbasova et al., Results in Physics. 12, 2202 (2019), doi: 10.1016/j.rinp.2019.02.068
[6] G.R. Gilmore., 2nd Edition, Wiley-VCH Verlag, Wenheim, Germany,(2008), ISBN 978-0-470-86196-7
[7] D. K. Gaikwad et al., Radiat. Phys. Chem. 138, 75 (2017), doi: 10.1016/j.radphyschem.2017.03.040
[8] P.P. Pawar et al., Radiat. Phys. Chem. 92, 22 (2013), doi: 10.1016/j.radphyschem.2013.07.004
[9] V.P. Singh et al., Radioprotection, 53, 145 (2018), doi: 10.1051/radiopro/2018008
[10] A. H. Taqi et al., J. Radiat. Res. Appl. Sc. 10, 252 (2017), doi: 10.1016/j.jrras.2017.05.008
[11] M.W. Marashdeh et al., Results in Physics, 5, 228 (2015), doi: 10.1016/j.rinp.2015.08.009
[12] B.M. Ladhaf et al., Radiat. Phys. Chem. 109, 89 (2015), doi: 10.1016/j.radphyschem.2014.12.015
[13] D. Demir et al., Ann. Nucl. Energy. 48, 17 (2012), doi: 10.1016/j.anucene.2012.05.013
[14] M. Kurudirek et al., Radiat. Phys. Chem. 78, 751 (2009), doi: 10.1016/j.radphyschem.2009.03.070
[15] K. Kirdsiri et al., Ann. Nucl. Energy. 38, 1438 (2011), doi: 10.1016/j.anucene.2011.01.031
[16] A.M. Zoulfakar et al., Appl. Radiat. Isotopes. 127, 269 (2017), doi: 10.1016/j.apradiso.2017.05.007
[17] K.S. Mann et al., Nucl. Eng. Technol. 49, 792 (2017), doi: 10.1016/j.net.2016.12.016
[18] R.R. Bhosale et al., Nucl. Techn. Radiat. Prot. 32, 288 (2017), doi: 10.2298/NTRP1703288B
[19] S. M. Vahabi, Vacuum. 136, 73 (2017), doi: 10.1016/j.vacuum.2016.11.011
[20] K.S. Mann et al., Radiat. Phys. Chem. 106, 247 (2015) doi: 10.1016/j.radphyschem.2014.08.005
[21] O. Gurler et al., Acta Phys. Pol. A. 130, 236 (2016), doi: 10.12693/APhysPolA.130.236
[22] N.B.J. Traynor et al., Appl. Spectrosc.72, 591 (2018), doi: 10.1177/0003702817745071
[23] M.F. Zaki et al., J. Lumin. 132, 119 (2012), doi:10.1016/j.jlumin.2011.08.001
[24] M.Y. Shoeib et al., Beni-Seuf Univ. J. Appl. Sci. 3, 74 (2014), doi: 10.1016/j.bjbas.2014.02.010
[25] F. Sen et al., American Journal of Optics and Photonics, 2, 7 (2014), doi: 10.11648/j.ajop.20140201.12
[26] J.H. Hubbell et al., National Institute of Standards and Technology (NIST), Gaithersburg, MD 20899, USA, NISTIR 5632 (1995)
[27] L. Gerward et al., Radiat Phys. Chem. 71, 653 (2004) doi:10.1016/j.radphyschem.2004.04.040
[28] M.J. Berger et al., 1987/99. Web Version 1.2, available at http:// physics.nist.gov/xcom . National Institute of Standards and Technology (NIST), Gaithersburg, MD 20899, USA, NBSIR 87-3597 (1987/99).
[29] R. Mirji et al., Radiat. Phys. Chem. 135, 32 (2017), doi: 10.1016/j.radphyschem.2017.03.001
[30] S. N. Ahmed. Academic Press Inc. Published by Elsevier, UK (2007), ISBN–13: 978-0-12-045581-2
[31] S. Agostinelli et al., Nucl. Instr. Meth. Phys. Res. A. 506, (2003), doi: 10.1016/S0168-9002(03)01368-8
[32] J. Allison et al., IEEE Transactions on Nuclear Science 53, (2006), doi: 10.1109/TNS.2006.869826
[33] J. Allison et al., Nucl. Instr. Meth. Phys. Res. A. 835, (2016), doi: 10.1016/j.nima.2016.06.125
[34] A. Kumar., Radiat. Physc. Chem., 127, 48 (2016), doi: 10.1016/j.radphyschem.2016.06.006
[35] M.L. Taylor et al, Med. Phys. 39, 1769-1778 (2012), doi: 10.1118/1.3689810

Licensed under a Creative Commons Attribution-NonCommercial-NoDerivatives 4.0 International License.

http://epublishing.ekt.gr | e-Publisher: EKT | Downloaded at 20/09/2021 19:03:40 |